# SPATIAL INTERPOLATION OF THE MOMENT MATRIX FOR EFFICIENT ANALYSIS OF MICROSTRIP CIRCUITS

*Todd W. Nuteson, Krishna Naishadham* and *Raj Mittra* *

Department of Electrical Engineering
Wright State University
Dayton, OH 45435

*Electromagnetic Communications Laboratory
University of Illinois
Urbana, IL 61801-2991

**Abstract**

An efficient moment method technique, based on spatial interpolation of the moment matrix, is developed for the analysis of microstrip circuit elements of arbitrary shape. Redundant calculations in the moment matrix are eliminated by utilizing various symmetries. The quasi-dynamic approximations of the Green's functions and closed-form analytical approximations of the Sommerfeld integrals are invoked to simplify the analysis. Sample computed results are presented on the current distribution obtained by interpolation of the moment matrix and agree very well with those evaluated without interpolation.

## I. INTRODUCTION

Microstrip elements occur in monolithic microwave and millimeter-wave integrated circuits (MMICs) to facilitate various circuit objectives. Computational methods based on full-wave analysis are generally used to solve accurately the current distribution or the fields associated with the circuit, thereby characterizing in terms of S-parameters and equivalent circuits, the parasitic effects, such as radiation, surface wave coupling, metallization and dielectric losses. These methods include the method of moments (MoM), the finite element method, the finite difference – time domain (FD-TD) method, and the transmission line matrix (TLM) method. For dense circuits, full-wave methods, in spite of their versatility to handle various geometries and material parameters, have the disadvantage of formidable memory requirements and CPU time. Therefore, it is desirable to investigate means of improving the efficiency of full-wave methods so that a circuit of moderate complexity and size can be analyzed in reasonable time. This paper describes an efficient MoM technique for the analysis of planar microstrip elements of arbitrary shape, based on reducing the computation time by spatial interpolation of the impedance matrix elements, and by utilizing various symmetries in the problem formulation. Efficiency is further enhanced by utilizing quasi-dynamic Green's functions [1], and the recently developed closed-form microstrip Green's functions [2], [3].

The interpolation method and the efficient matrix-fill scheme are illustrated with reference to computation of the current distribution on a rectangular microstrip patch deposited on thin as well as thick substrates. The current distribution obtained by interpolation compares very well with that without interpolation. The proposed method has been applied to calculate the S-parameters of meander lines and spiral inductors, and agrees reasonably well with measurements [4].

## II. FORMULATION

### A. *Moment Method*

The boundary value problem for the current distribution on the surface of the conductor is formulated as a Mixed (scalar and vector) Potential Integral Equation (MPIE) [1]. The microstrip surface is segmented into rectangular cells, and rooftop basis functions and the razor testing procedure are employed to compute the current distribution in each cell. A coaxial probe with its center conductor embedded in the dielectric substrate is used as excitation for the currents [1]. From the current distribution, the multiport impedance matrix and the scattering (S) parameters of the discontinuity are computed. Application of the MoM to the MPIE results in a matrix equation in which the elements of the matrix consist of scalar and vector potential integrals defined over the support of a pulse function and a rooftop basis function, respectively. The reader is referred to [4] for expressions of the impedance matrix elements and the excitation vector for a coax probe.

### B. *Efficiency Considerations*

#### B.1. *Efficient Matrix Fill*

The redundancies present in the moment matrix for equal size cells, chosen here for convenience, can be taken advantage of in reducing the matrix fill-time. A careful examination of the matrix elements reveals (upto) a sixteen-fold redundancy for the scalar potential contributions, manifested by the overlapping of the rooftop basis functions [4]! Therefore, a significant reduction in the matrix fill time can be achieved by computing each scalar potential integral and placing it in the appropriate matrix element as it is calculated. Similar considerations apply to the vector potential integrals.

The Green's functions depend on the distance $R = |\rho - \rho'|$ between source and observation points. Depending on the trace geometry being examined, there may be only a few distinct source-observer distances. For example, on a rectangular patch divided into m×n charge cells (Fig. 1), there are only mn such distances, or equivalently, mn dis-

OF2



CH3277-1/93/0000-0971$01.00 © 1993 IEEE

tinct scalar potential integrals, (m–1)n distinct integrals for the x–directed vector potential, and (n–1)m distinct integrals for the y–directed vector potential. Filling the moment matrix without utilizing any symmetry involves the computation of $(2mn - m - n)^2$ potential integrals, in contrast to the $(3mn - m - n)$ integrals required in our efficient fill–in scheme. Therefore, we could precompute and store these $(3mn - m - n)$ distinct potentials in a two–dimensional array (called the storage matrix), and retrieve them later to fill the entire moment matrix. Considerable time and memory savings can be accomplished in this manner. In order to compute these distinct potentials, we may place the source on any cell (say, cell (1,1) — see Fig. 1), move the observation point through all the cells, and compute the potential integrals. The computational efficiency is further enhanced by interpolating the Green's functions [1].

The efficient matrix fill scheme described above for a rectangular patch may be used even if the circuit boundary does not conform to a rectangle. For example, consider the spiral inductor geometry shown in Fig. 2. The hatched cells (except cell (1,1)) correspond to the conductor (or metal). Unhatched cells are non–metallic. Using symmetries within the rectangular boundary, we could place the source current of 1 A on cell (1,1) and compute all the distinct source – observer interactions, including those pertaining to non–metallic cells. From these interactions, we could select only those which represent metallic cell interactions. A considerable time savings can be obtained in spite of the extra calculations involving non–metallic cells. If the inductor geometry is changed keeping the cell size unaltered, there is no necessity to compute any more interactions, since all the interactions are already available from the primary rectangle.

In Fig. 3, we compare the CPU time required for an efficient fill of the moment matrix using the method discussed above, with the time involved in filling the complete matrix without the utilization of any symmetry. The structure investigated is a square patch of side 75 mm deposited on 100 $\mu$m thick GaAs substrate. For large matrix orders, the CPU time for the complete matrix fill (or **CMF**) is at least one order of magnitude higher than the time required for the efficient matrix fill (or **EMF**). As an example, to fill a 500 × 500 matrix, the CMF requires 2000 (s) whereas the EMF takes about 100 (s). For comparison, the time involved in inverting the moment matrix by standard LU decomposition is also plotted as a function of matrix order. The time required for CMF is **higher** than the inversion time by one to two orders of magnitude. By extrapolation to large matrix orders, this dominance of the CMF time is expected to continue until the order becomes 5000 or so. However, the EMF requires times much less than the inversion times, especially for large matrix orders. The EMF time can be reduced even further by interpolating the matrix elements as a function of the distance between the source and observation cells, as we show next.

*B.2. Interpolated Efficient Matrix Fill (IEMF)*

The IEMF method involves computation of only those potential integrals in the storage matrix which correspond to source and observation cells in close proximity. These are the dominant terms in the matrix. The remainder of the matrix elements are spatially interpolated from these sampled values of the potential integrals by using cubic splines. This improvement would enhance the efficiency of the EMF technique considerably, since only a few terms of the matrix are computed directly, and the remainder, i.e., a significant majority of the matrix, is computed by closed–form interpolation. Next, we shall illustrate with an example the improvements possible with the IEMF method.

Consider the rectangular patch shown in Fig. 1, divided into m×n cells, each of dimensions $\Delta x=L/m$ and $\Delta y=W/n$. To fill the storage matrix for the scalar potential using the IEMF operation, the source of unit charge is placed in cell (1,1) and the interactions of the source cell with all the cells, including the self-contribution, are computed. These interactions, given by (see Fig. 1a)

$$V_{ij} = \int_{y_0}^{y_1}\int_{x_0}^{x_1} G_V(\rho_{ij};\, \rho')\, dx'dy', \qquad i = 1,2,...,m;\ j = 1,2,...,n \tag{1}$$

are parametrized with respect to the distance

$$R_{ij} = |\rho_{ij} - \rho'_{11}| = \sqrt{(x_i - x_1)^2 + (y_j - y_1)^2} \tag{2}$$

between the centers of the source and observation cells for interpolation purposes. Instead of calculating all the mn interactions, as done in EMF, the IEMF operation samples only those integrals corresponding to the source in cell (1,1) and the observation point centered in cells (i,1), i=1,2,...m, i.e., along the first row, in cells (k,k), k=2,3,...n, i.e., along the main diagonal, and at a few other observation points whose number depends on the polar angle, $\phi(0 < \phi < \pi/4)$, of the radius vector between the source and observation points (see Fig. 1a). For the example in Fig. 1a, a total of m + n + 3 samples of the scalar potential integrals would be calculated in the IEMF method.

An approach similar to that used for the scalar potential also applies to the vector potential integrals. For example, for the x–directed vector potential, the interaction between the basis function $\Omega_{11}(x',y')$ spanning the first two cells (Fig. 1b) and observation points along a test path centered at $(x_p,\ y_j - \Delta y/2)$ needs to be considered. This interaction, given by

$$A_{x_{pj}} = \int_{x_p - \frac{\Delta x}{2}}^{x_p + \frac{\Delta x}{2}} \int_{y_0}^{y_1}\int_{x_0}^{x_2} G_A(\rho_{pj};\, \rho')\, \Omega_{11}(x',y')\, dx'dy'dx, \qquad p = 1,2,...,m-1, \qquad j = 1,2,...,n \tag{3}$$

is parametrized, for interpolation, in terms of the "mean" distance (see Fig. 1b)

$$D_{x_{pj}} = \tfrac{1}{3}(d_{x_1} + d_{x_2} + d_{x_3}) \tag{4}$$

where

$$d_{x_1} = \sqrt{\left[x_p - \frac{\Delta x}{2} - x_1\right]^2 + (y_j - y_1)^2} \tag{5a}$$

$$d_{x_2} = \sqrt{(x_p - x_1)^2 + (y_j - y_1)^2} \tag{5b}$$

$$d_{x_3} = \sqrt{\left[x_p + \frac{\Delta x}{2} - x_1\right]^2 + (y_j - y_1)^2} \tag{5c}$$

With reference to Fig. 1b, a total of 2(m + n + 3) samples of the x– and y–directed vector potential integrals would be calculated to fill the storage matrices of the vector potential by the IEMF method.

In Table I, we compare the number of calculations of the potential integrals in the EMF and IEMF methods as a function of the order N of the moment matrix. It is observed that significant savings (e.g., 90% at N = 1000) in the number of calculations can be accomplished by using the IEMF method.

## IV. CONCLUSIONS

An efficient full–wave moment method, involving spatial interpolation of the moment matrix, has been developed for the analysis of microstrip circuit elements of arbitrary shape. Several techniques have been used to increase the efficiency of the algorithm, including the utilization of (a) the closed–form microstrip Green's functions, and (b) various symmetries in the problem formulation, which facilitate an efficient fill–in of the moment matrix. Using interpolation to fill the moment matrix has proven to be very efficient and produces negligible error in the current distribution for off–resonant frequencies. This method is not valid for resonant structures where the accuracy of every matrix element becomes crucial.

The IEMF method can be applied to fill the moment matrix for any arbitrary planar circuit geometry, which can be contained within a rectangle, and which can be represented accurately by rectangular cell division. This method allows the geometry to be changed without having to recalculate the scalar and vector potential integrals, and is therefore, much more efficient than defining a unique geometry for every structure.

Table I. Comparison of the number of potential integral calculations in the EMF and IEMF methods.

| Matrix order (N) | Total # of matrix elements | # of calculations using EMF ($N_E$) | # of calculations using IEMF ($N_I$) | % of elements needed to be calculated in IEMF ($N_I/N_E$) × 100 |
|---|---|---|---|---|
| 0 | 1,600 | 65 | 35 | 54 |
| 1,012 | 1,024,144 | 1,541 | 144 | 9.5 |
| 4,900 | 24,010,000 | 7,400 | 306 | 4 |

## III. RESULTS

We now present sample results on the accuracy of the current distribution obtained by using the IEMF method. Fig. 4 shows, as a function of frequency, the average percentage error in the current distribution, defined as

$$\% \text{ error} = \frac{1}{N}\sum_{i=1}^{N}\left[\frac{I_{i,EMF} - I_{i,IEMF}}{I_{i,EMF}}\right] \times 100 \qquad (6)$$

where N = (m – 1)n + m(n – 1), for the real and imaginary currents on a square patch of side 7.5 mm, deposited on a GaAs substrate of thickness h = 100 $\mu$m and dielectric constant $\epsilon_r$ = 12.85. The patch is divided into 10×10 square cells, and is excited by a coax probe centered in cell (1,1). The patch is resonant at a frequency of 5.23 GHz, where a large error (15% for the real and 50 % for the imaginary currents) occurs. However, at frequencies off resonance, the error in both real and imaginary currents is reduced to less than 0.1%. Only the first resonance is shown in Fig. 4, but the pattern of large errors in the currents recurs at subsequent resonant frequencies.

Fig. 4 shows the average error in the current for a thin substrate. In Fig. 5, we display the percentage error in the currents computed by using the IMEF method for a square patch of side 80 mm on a glass epoxy substrate ($\epsilon_r$ = 4.7, h = 64 mils) — a relatively thick substrate. The cell division and the coax probe location are the same as those for Fig. 4. The first resonance of this structure occurs at 864.87 MHz. This structure shows the same pattern as the previous case, where the error is large close to resonance and less than 0.1% off resonance.

The IEMF method has been applied to the calculation of S–parameters of typical microstrip transmission line discontinuities and passive circuit elements, including meander lines and spiral inductors. Good agreement has been observed between our computed results and those obtained from commercial software packages as well as experiments on a vector network analyzer [4].

## REFERENCES


[1] J. R. Mosig, "Integral Equation Technique," in *Numerical Techniques for Microwave and Millimeter-Wave Passive Structures*, (T. Itoh, ed.), John Wiley, New York, pp. 133–213, 1989.

[2] Y. L. Chow, J. J. Yang, D. G. Fang, and G. E. Howard, "A closed–form spatial Green's function for the thick microstrip substrate," *IEEE Trans. Microwave Theory Tech.*, vol. MTT–39, no. 3, pp. 588–592, 1991.

[3] M. I. Aksun and R. Mittra, "Investigation of radiation characteristics of microstrip etches," Technical Report No. UILU–ENG–92–2210, University of Illinois at Urbana–Champaign, March 1992.

[4] K. Naishadham and T. W. Nuteson, "Moment method analysis of arbitrarily shaped planar microstrip discontinuities," Final Report for Contract No. F33615–90–C–1405 between Wright State University and SCEEE, May 31, 1992.

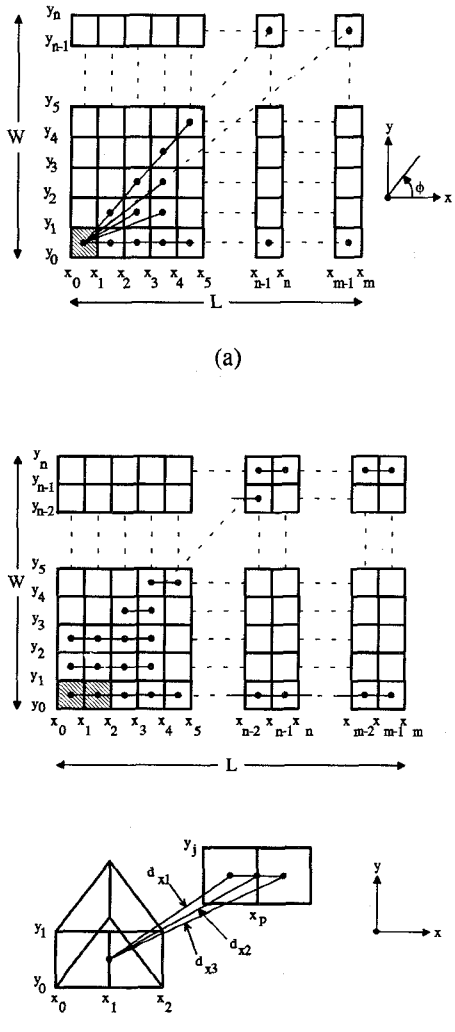


Fig. 1 (a) The match point locations for scalar potential integrals computed in IEMF. (b) The test path locations for vector potential integrals. The source is placed in the hatched cells.

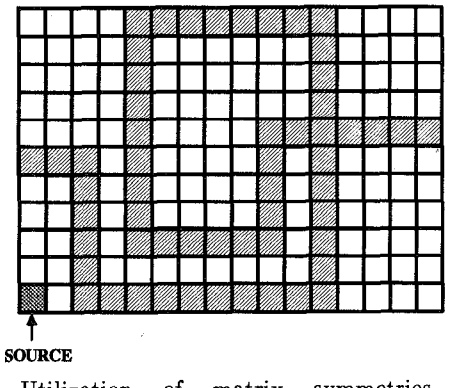


Fig. 2 Utilization of matrix symmetries (EMF method) for a spiral inductor.

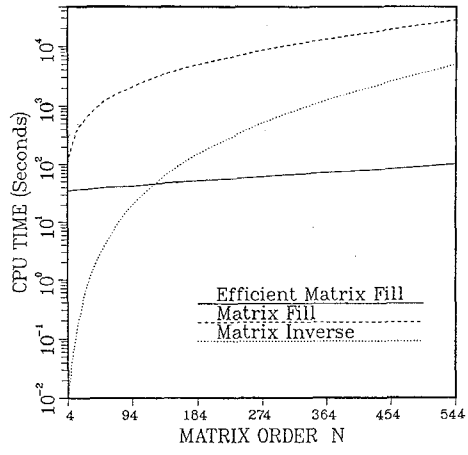


Fig. 3 Comparison of moment matrix fill and inversion times on VAX–8550 computer as a function of matrix order.

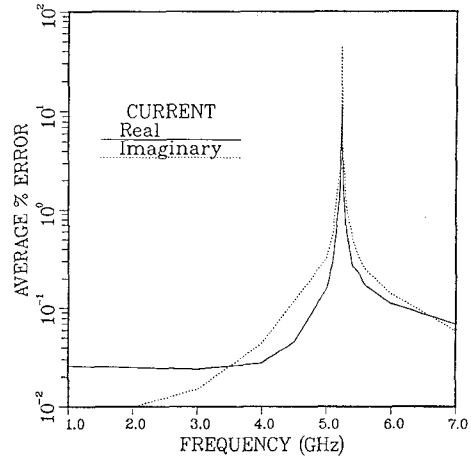


Fig. 4 Error in the real and imaginary currents computed by IEMF for a thin substrate.

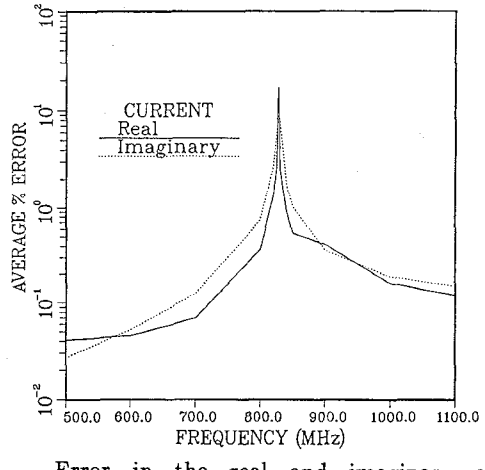


Fig. 5 Error in the real and imaginary currents computed by IEMF for a thick substrate.